

Dental Materials

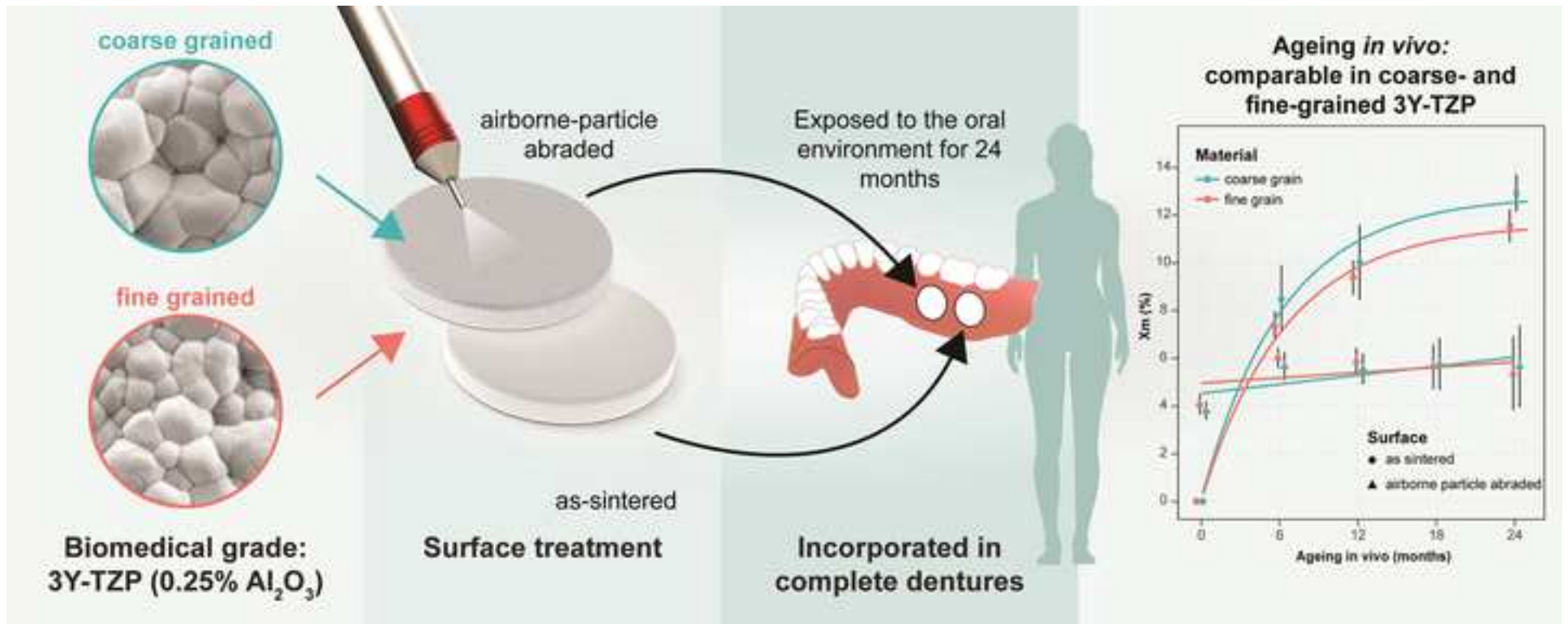
In vivo ageing of zirconia dental ceramics – Part I: biomedical grade 3Y-TZP

--Manuscript Draft--

Manuscript Number:	DENTMA-D-20-00884
Article Type:	Full Length Article
Keywords:	Zirconia ceramics; 3Y-TZP; Low-temperature degradation; in vivo ageing; airborne-particle abrasion; Transformation zone depth; XRD; FIB-SEM
Corresponding Author:	Peter Jevnikar University of Ljubljana Medical Faculty Ljubljana, Slovenia
First Author:	Andraž Kocjan
Order of Authors:	Andraž Kocjan Jasna Cotič Tomaž Kosmač Peter Jevnikar
Abstract:	<p>Objective. In vivo ageing of biomedical grade 3Y-TZP ceramics in the oral environment was assessed and compared to artificially accelerated in vitro hydrothermal ageing extrapolations at 37°C.</p> <p>Methods. 88 discs were pressed and sintered (1450-1500°C) from two commercial 3Y-TZP compositions containing 0.25% Al₂O₃ to generate finer- and coarser-grained specimens. As-sintered (AS) and airborne-particle abraded (APA; 50 µm Al₂O₃) surfaces were investigated. In vivo ageing was performed by incorporating specimens were incorporated in lingual flanges of complete dentures of 12 edentulous volunteers who wore them continuously for up to 24 months. For comparison, in vitro hydrothermal aging at 134°C was also performed and analysed by XRD and (FIB)-SEM. Data was statistically analysed with linear and asymptotic regression models.</p> <p>Results. Finer and coarser-grained specimens exhibited statistically insignificant differences in ageing in vivo. The monoclinic fraction (X_m) on AS surfaces increased to ~8% after 6 months. The ageing process then decelerated, settling at ~0.24%/month. After 24 months, X_m reached ~12%. The maximum calculated transformed layer was 0.385 µm representing one layer of transformed grains. APA surfaces were significantly more ageing resistant. The initial X_m of ~4.0% linearly increased by 0.04%/month in vivo. In vitro ageing exhibited more uniform, linear ageing kinetics. Coarser-grained AS surfaces aged significantly faster than fine-grained (2.27%/h compared to 1.96%/h). APA discs aged at a rate of 0.4%/h in vitro. Microcracking within a single grain and pull-out of grain clusters were observed on aged AS surfaces.</p> <p>Significance. Biomedical grade 3Y-TZP was susceptible to in vivo ageing. After 2 years in vivo, the ageing kinetics were almost 3-times faster than the generally accepted in-vitro-in-vivo extrapolation.</p>

Highlights:

- *In vivo* ageing kinetics was assessed for biomedical grade 3Y-TZP ceramics.
- 2-year exposure showed ~3-times faster ageing kinetics compared to *in vitro* extrapolation.
- Airborne-particle abrasion significantly suppresses *in vivo* ageing.
- Surface degradation after 2-year *in vivo* was within clinically acceptable range.



In vivo ageing of zirconia dental ceramics – Part I: biomedical grade 3Y-TZP

Andraž Kocjan^a, Jasna Cotič^b, Tomaž Kosmač^a, Peter Jevnikar^{b,}*

^a Department for Nanostructured Materials, Jožef Stefan Institute, Jamova 39, SI-1000 Ljubljana, Slovenia

^b Department of Prosthodontics, Faculty of Medicine, University of Ljubljana, Hrvatski trg 6, SI-1000 Ljubljana, Slovenia

* Corresponding author: Peter Jevnikar, Department of Prosthodontics, Faculty of Medicine, University of Ljubljana, Hrvatski trg 6, SI-1000 Ljubljana, Slovenia.

E-mail: peter.jevnikar@mf.uni-lj.si

In vivo ageing of zirconia dental ceramics – Part I: biomedical grade 3Y-TZP

Objective. *In vivo* ageing of biomedical grade 3Y-TZP ceramics in the oral environment was assessed and compared to artificially accelerated *in vitro* hydrothermal ageing extrapolations at 37°C.

Methods. 88 discs were pressed and sintered (1450-1500°C) from two commercial 3Y-TZP compositions containing 0.25% Al₂O₃ to generate finer- and coarser-grained specimens. As-sintered (AS) and airborne-particle abraded (APA; 50 µm Al₂O₃) surfaces were investigated. *In vivo* ageing was performed by incorporating specimens were incorporated in lingual flanges of complete dentures of 12 edentulous volunteers who wore them continuously for up to 24 months. For comparison, *in vitro* hydrothermal aging at 134°C was also performed and analysed by XRD and (FIB)-SEM. Data was statistically analysed with linear and asymptotic regression models.

Results. Finer and coarser-grained specimens exhibited statistically insignificant differences in ageing *in vivo*. The monoclinic fraction (X_m) on AS surfaces increased to ~8% after 6 months. The ageing process then decelerated, settling at ~0.24%/month. After 24 months, X_m reached ~12%. The maximum calculated transformed layer was 0.385 µm representing one layer of transformed grains. APA surfaces were significantly more ageing resistant. The initial X_m of ~4.0% linearly increased by 0.04%/month *in vivo*. *In vitro* ageing exhibited more uniform, linear ageing kinetics. Coarser-grained AS surfaces aged significantly faster than fine-grained (2.27%/h compared to 1.96%/h). APA discs aged at a rate of 0.4%/h *in vitro*. Microcracking within a single grain and pull-out of grain clusters were observed on aged AS surfaces.

Significance. Biomedical grade 3Y-TZP was susceptible to *in vivo* ageing. After 2 years *in vivo*, the ageing kinetics were almost 3-times faster than the generally accepted *in-vitro-in-vivo* extrapolation.

Keywords: Zirconia ceramics, 3Y-TZP, Low-temperature degradation, *in vivo* ageing, airborne-particle abrasion, Transformation zone depth, XRD, FIB-SEM

1. Introduction

In the past three decades, there have been major advances in the application of 3 mol.% yttria partially stabilized zirconia polycrystalline (3Y-TZP) ceramics for dental restorations. This is due to their superior mechanical properties compared to other, especially glass-based dental ceramics [1]. 3Y-TZP's high strength and fracture toughness are governed by the stress-induced transformation (*t*-*m*) toughening mechanism, where under applied stress the metastable tetragonal phase transforms to monoclinic. This causes volumetric expansion and creates compressive stresses that oppose the tensile stress in the vicinity of a propagating crack tip [2][3]. Transformation toughening has made 3Y-TZP an attractive alternative to traditionally used metals and led to its use for all-ceramic prosthodontic restorations, post-and-core systems and dental implants.

3Y-TZP's tetragonal phase metastability also has a well-documented, deleterious aspect known as low-temperature degradation (LTD) or ageing [4][5]. In humid environments, the *t*-*m* transformation can be triggered spontaneously [6][7]. This nucleation and growth process initiates from isolated surface grains and gradually proceeds into the bulk via a stress-corrosion-type mechanism [6][8][9]. The growth rate appears to be linear without any retardation or limit [10][11]. The transformed zone is a gradientless layer with an amount of residual non-transformed zirconia separated from unaffected material by a clear boundary [10][11][12]. The accepted mechanistic theory states that the negatively charged water species annihilate the oxygen vacancies, destabilizing the *t*-ZrO₂ domains [13][14]. The mechanism leading to the *t*-*m* transformation is thus temperature-dependent and diffusion-controlled, while the *t*-*m* phase transformation, once nucleated, is martensitic and is accompanied by extensive micro-cracking, which ultimately leads to strength degradation [15].

At the onset of the present millennium, several hundreds of 3Y-TZP femoral heads failed in a short period following implantation, with the origin of the fracture indirectly associated with hydrothermal degradation [16][17]. Since then, extensive studies have been conducted to investigate the ageing mechanisms and kinetics, resulting in a general definition of the

conditions when LTD is prone to occur. Hydrothermally-induced transformation of 3Y-TZP ceramics is known to be a grain-size dependent process [18][9][19], which can be further influenced by composition, chemical and microstructural inhomogeneities [20][4], materials background and treatment (i.e. surface mechanical/thermal/chemical modifications) [21][22][23][24][25] and/or testing conditions [10][26]. The role of the aqueous medium is not entirely clear, but will likely influence the transformation rate [27]. The same holds for the influence of mechanical surface treatment.

Ageing kinetics of 3Y-TZP ceramics were commonly investigated using accelerated hydrothermal protocols in autoclaves. According to Deville and Chevalier [28][29], the relationship between the amount of transformed monoclinic phase and the ageing time at various temperatures can be used as guidance to estimate the equivalent ageing time under “*in vivo*” conditions. Based on results obtained from failed zirconia femoral heads, these authors have calculated that 8 hours of accelerated ageing in an autoclave at 134°C in distilled water, should result in ~35% of the monoclinic fraction and correspond to approximately 32 years *in vivo* for this particular material and application. However, this generally accepted *in-vitro-in-vivo* extrapolation has been shown to be a major underestimation of the ageing process.

Namley, Keuper et al. who studied LTD of 3Y-TZP at 37°C and normal pressure conditions showed that ~35% of the transformed surface layer (~0.5 µm per year) was obtained after only 4 years, which is 8-times faster than according to the above mentioned *in-vitro-in-vivo* extrapolation [30]. Accelerated ageing also suffers from known reproducibility complications when using different autoclaves, as water vapour pressure is a decisive factor for the transformation rate [10]. Therefore, studying *in vivo* ageing behaviour in the oral environment is mandatory to better understand its real-time behaviour and severity. Literature, however, remains remarkably scarce on this subject. A short, intra-oral ageing study by Miragaya et al. reported that 60 days of ageing already resulted in the evolution of 4.7–7.7 wt.% of m-ZrO₂

and substantially affected flexural strength, Young's modulus, Vickers hardness and indentation toughness [31].

Our research group approached the problem by using complete dentures as vehicles to hold the zirconia ceramic specimens in patients' mouths during normal function. In this manner the ageing processes could be studied at body temperature in the aggressive environment of the oral cavity. Flat specimens allowed for easy removal and good patient compliance, which enabled us to conduct thorough microstructural and crystallographic analyses over the course of several years. The results were extensive and we decided to report them in two co-published articles, this being the first of the two [ref in vivo paper 2]. This study was designed to monitor the propagation of the *t-m* transformation of two biomedical grade, classic zirconia ceramics containing 0.25 wt.% of alumina differing in their mean grain size and transformability. The aim was to assess the extent of *in vivo* ageing behaviour in the oral environment, compare it to *in vitro* hydrothermal ageing and assess their relationship with the established ageing extrapolations at 37°C [24][44].

2. Material and methods

2.1. Specimen preparation

Two high-purity "bio-medical-grade" powders TZ-3YB-E and TZ-3YSB-E, from Tosoh, Japan, were used to produce disc-shaped specimens (7.8 mm in diameter and 0.8 mm thick), which were labelled as B-E and SB-E, respectively. The discs were formed by uni-axial dry-pressing at 150 MPa. Due to their higher surface area the finer B-E pressed compacts were sintered at 1450°C resulting in a nearly theoretical density (>99% TD), whereas a higher sintering temperature of 1500°C was needed to reach a similarly high relative density of the coarser SB-E pressed compacts. After sintering, specimens from each material were divided into four groups of ten. Two groups of each material were left as-sintered (AS) and two groups were sandblasted or airborne-particle abraded (APA). The FEG-SEM micrographs illustrate the characteristic topography of the AS surfaces, whereas the grooves mimick those produced with the CAD/CAM technique (Fig. 1a). After sintering, the AS B-E and SB-E specimens

exhibited mean grain sizes of 0.59 μm and 0.51 μm , respectively (Figs. 1b-c). Air particle abrasion was performed at a distance of 30 mm for 15 seconds with 50- μm fused alumina particles at 2.5 bar, since this is a preferential method to clean the cementation surface and to increase surface roughness (Fig. 1d) for improved bonding with luting cements [49].

2.2. *In vivo* ageing protocol

The *in vivo* ageing experiment was based on the participation of 12 healthy volunteers (9 men and 3 women) willing to have the ceramics specimens incorporated into their complete dentures. The participants were recruited from the pool of edentulous patients treated with complete dentures at the Department of Prosthodontics, Faculty of Medicine, University of Ljubljana. The following criteria were used to select the patients: good rating of the existing dentures based on the visual scale questionnaire, dentures worn 24h/day, no head and neck radiotherapy. Patients received verbal and written information on the study design and gave signed consent to participate.

The study was approved by the National Medical Ethic Committee of the Republic of Slovenia. (approval no. 61/04/1011). All the procedures were in accordance with the Helsinki Declaration of 1975. Disc-shaped cavities were prepared in the lower complete denture of each participant with a tungsten-carbide bur no (SH 72E, Shofu, Japan). Two fine-grained and two coarse-grained discs were implanted in the lingual flange of the lower denture with the abraded or as-sintered surface exposed to the oral environment. Cold cured acrylic resin (Ivoclar, Liechtenstein) was used to fix the 3Y-TZP specimens in the dentures (Figs. 1f-h). The retention and stability of dentures were checked and patients reported no discomfort at the insertion of this newly constructed intraoral device.

Volunteers were instructed to remove the dentures for cleaning twice a day using a soft toothbrush and soapy water. They were also instructed to wear the dentures continuously for 24h/day and not to use any additional mouthwash or denture cleaner for the duration of the study. After 6 months the discs were explanted, gently cleaned by ultrasonication in sodium

hypochlorite to remove the adhered proteins and subjected to XRD and FEG-SEM surface analyses. The visits were part of a regular recall program to check the function of the dentures. After analyses were complete, the specimens were re-implanted with cold-curing acrylic resin for the next 6-month period. The same protocol was followed until the end of the study at 24 months.

For comparison, specimens of each material and surface treatments were exposed to accelerated artificial ageing by autoclaving in an artificial saliva under isothermal conditions at 134 °C for 10 hours.

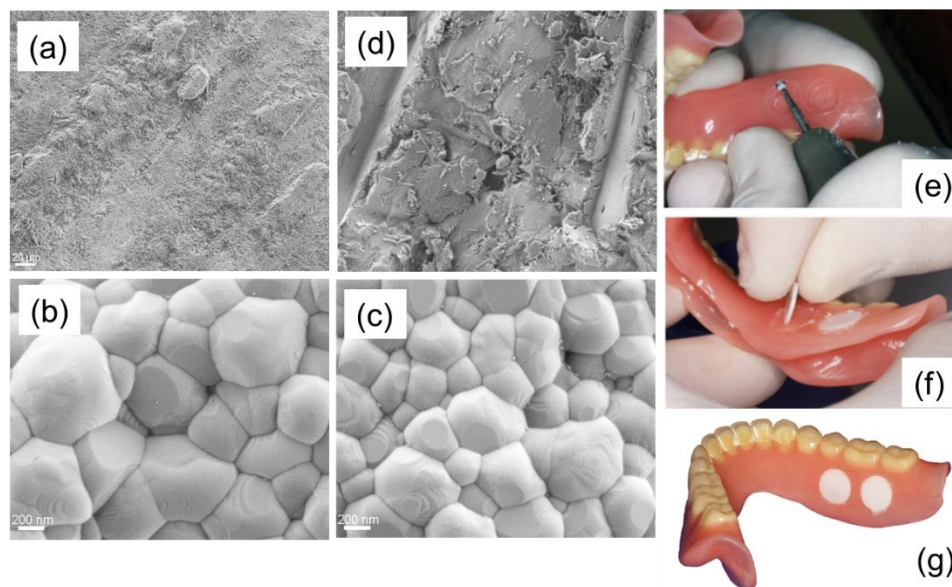


Figure 1. Experimental design. Low-magnification SEM micrograph of the 3Y-TZP sample surface showing uneven, jagged features induced by using roughened steel punches of the mould for dry pressing to mimic the surface roughness introduced with CAD/CAM machining (a). High-magnification SEM micrographs showing coarser and finer microstructures of the SB-E and B-E 3Y-TZP samples, respectively (b, c). Airborne particle abrasion resulted in substantial surface damage with sharp cuts from the impacts of alumina particles (d). To mount the ceramic specimens in the dentures, disc shaped slots were prepared (e) and filled with cold-curing acrylic resin. The specimens were positioned so that the treated side was exposed to the oral cavity (f). The experimental intraoral ageing device consisted of a complete denture with 3Y-TZP ceramic specimens inserted in sublingual flanges (g).

2.3. *In vitro* ageing protocol

Accelerated *in vitro* ageing was performed by autoclaving groups of 5 specimens in artificial saliva under isothermal conditions at 134°C for up to 10 hours.

2.4. *Specimen characterisation*

The microstructural observations were made by field emission scanning electron microscope (FE-SEM Carl Zeiss, Supra 35LV, Oberkochen, Germany) using accelerated voltage of 1 kV. Grain size evaluations were made on polished (3 µm diamond paste) and thermally etched (1380°C, 1 h), uncoated specimens, using the linear intercept method, based on the ASTM E112-13 standard without any correction factors used [32].

X-ray diffraction patterns (XRD) were collected from all the specimens from each group with X'Pert PRO X-Ray diffractometer equipped with a PIXcel detector using Cu-K α radiation at 45 kV and 40 mA over the range of 25–40° 2 θ (PANalytical, Almelo, The Netherlands). The relative amount of transformed monoclinic zirconia (m -ZrO₂) on the specimens' surfaces was determined from the integrated intensities of the monoclinic (1 $\bar{1}$ 1)_m and (111)_m, and the tetragonal (101)_t peaks according to the method of Garvie and Nicholson,[33] which can be applied to determine the phase composition of zirconia with randomly distributed m -ZrO₂ and t -ZrO₂ phases at any distance from the surface exposed to XRD. To generate additional information related to ageing kinetics, the thickness of the propagating transformed zone depth (TZD) layer was calculated in µm [37] based on the XRD data.

For the FIB-SEM analysis (FEI Helios Nanolab 650) the regular cross-sections were made using ion-beam machining and were finalized by ion polishing. Prior to machining and polishing, a 0.5 µm layer of platinum film was sputtered on the area of interest, using the ion-beam-assisted gas injection system at 30 kV and 0.43 nA to prevent the extensive curtain effect. As-prepared cross-sections were observed *in situ*, at an angle of 52°, using the electron probe at 2 kV and 100 pA.

2.5. Statistical analysis

Data on the monoclinic content was statistically analyzed with linear and non-linear regression models. Tukey's HSD test was used to examine the pairwise differences between treatment groups. The statistics software package R 3.1.2 was used for the analyses [R reference]. The significance level was set to $\alpha = 0.05$.

3. Results

The participants displayed good adherence to the study setup and reported no issues with wearing the experimental dentures. One participant withdrew due to ill health after 6 months, one was not able to continue participating after 12 months due to relocation and one was lost to follow-up after 18 months. Other participants were able to attend the visits as planned until the end of the study.

3.1. Diffractograms of the exposed specimen surfaces

According to the results of the XRD analysis, AS SB-E and B-E materials initially consisted of monoclinic-free t -ZrO₂ (Fig. 2a). In addition, a significant amount of t' -ZrO₂ (usually referred to simply as the cubic phase) was also present, as indicative by the small double peak positioned at 35° 2 θ in between the (002)_t and (110)_t peaks of t -ZrO₂. This phase can represent more than 21 % in the 2-hour-long sintering regimen at 1450-1500 °C [34].

After 6 months *in vivo*, XRD diffractogram of AS surfaces developed noticeable monoclinic peaks (m -ZrO₂) at 28.15°, 31.3° and 34°. They corresponded to (1 $\bar{1}$ 1)_m, (111)_m and (002)_m and indicated the initiation of the ageing process (Fig. 2a). With longer ageing times of 12 and 24 months, the intensity of the monoclinic peaks slightly increased, but not substantially. APA, on the other hand, resulted in more complex diffractograms commonly seen in mechanically damaged 3Y-TZP surfaces (Fig. 2b) [22][35]. These diffractograms exhibited much lower peak intensities due to uneven surfaces. In addition to the initial occurrence of the monoclinic phase (X_m) of about 4%, they also exhibited a low-2 θ -angle broadening of the main tetragonal peak

(101)_t, a reversed intensity of tetragonal doublet peaks (002)_t and (110)_t, at 35° 2θ, and an increased full width at half maximum (FWHM) of the (002)_t peak as compared to the (110)_t counterpart.

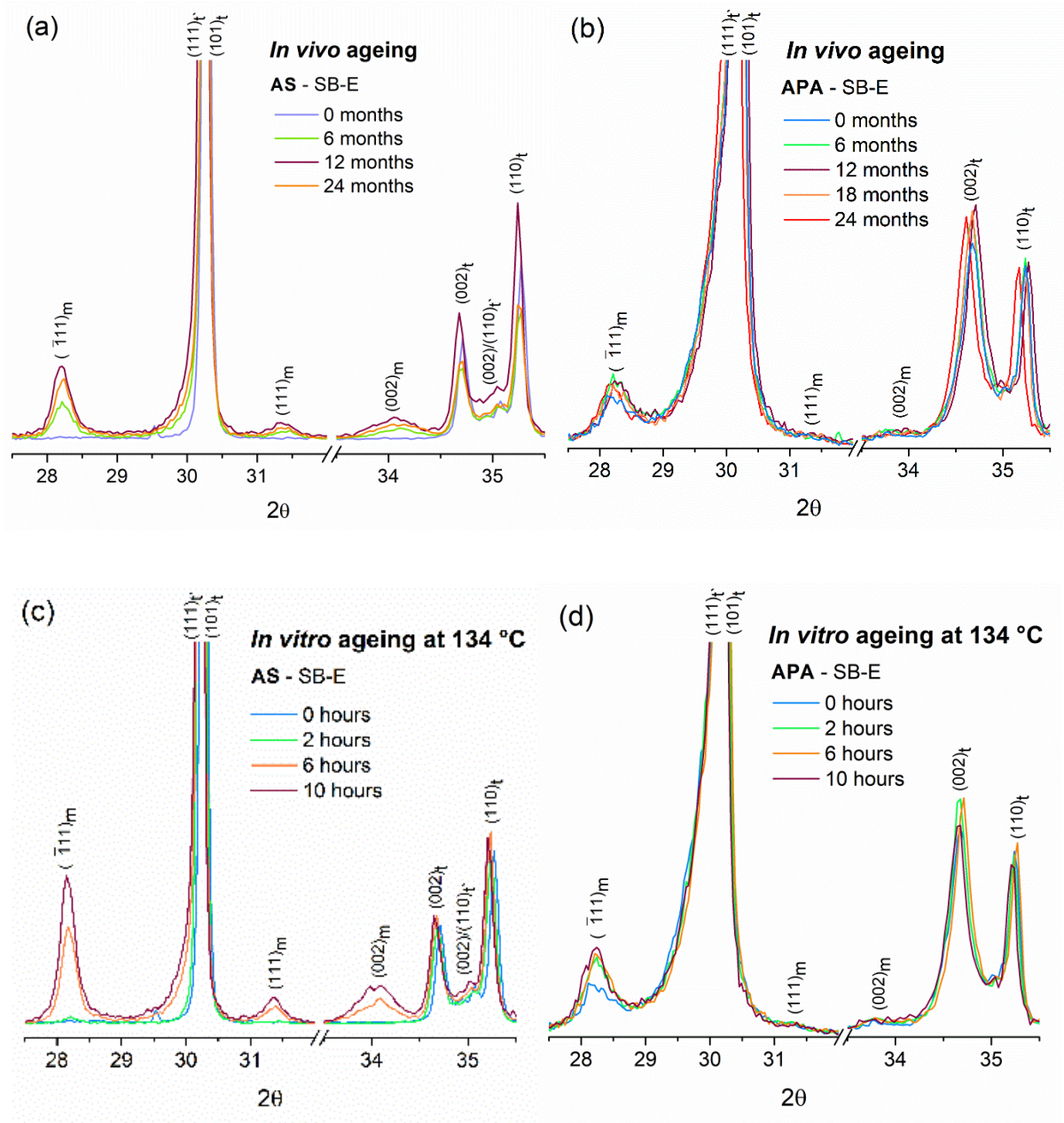


Figure 2. Ageing behaviour. Representative XRD patterns obtained from the as-sintered and sandblasted SB-E specimen surfaces that were aged up to 24 months *in vivo* (a, b) and up to 10 hours *in vitro* (c, d).

The diffractograms of AS specimens subjected to *in vitro* ageing in Figs 2c-d appear similar to the *in vivo* counterparts (Figs. 2a-b), but the dynamics of *t-m* transformation were different. In

AS SB-E specimens, there was only a slight emergence of the $(1\bar{1}1)_m$ monoclinic peak after 2 hours, suggesting the existence of an initial incubation period. After 6 and 10 hours *in vitro*, the intensities the *m*-ZrO₂ peaks already exceeded those encountered after 24 months *in vivo* (Fig. 2a).

APA specimens exhibited a visible initial increase of the $(1\bar{1}1)_m$ peak immediately after 2 hours *in vitro*. However, this remained practically unchanged for the subsequent 8 hours of ageing. An interesting observation was that the $(111)_m$ peak did not seem to increase at all. This is indicative of the preferred orientation of the formed monoclinic domains after APA. It was shown that when a large shear component is present, it causes a stress-induced preferred orientation of both tetragonal and monoclinic variants [36].

3.2. Analysis of the monoclinic fraction (X_m) and transformed zone depth (TZD)

The mean values for the transformed monoclinic fraction (X_m) with their respective standard deviations are summarized in Table 1 (*in vivo* ageing) and Table 2 (*in vitro* ageing).

Table 1. Mean values and standard deviations for the monoclinic content (X_m) before and after ageing *in vivo*. Values marked with the same letters are not significantly different from each other (Tukey's HSD test, $\alpha=0.05$). APA = airborne-particle abraded.

Ageing <i>in vivo</i> (months)	Material	Surface treatment	X_m in % (SD)
0	BE	as sintered	0.0 ⁱ (0.00)
0	SBE	as sintered	0.0 ⁱ (0.00)
0	BE	APA	4.1 ^{gh} (0.42)
0	SBE	APA	3.8 ^h (0.36)
6	BE	as sintered	7.3 ^e (0.61)
6	SBE	as sintered	8.5 ^{de} (1.40)
6	BE	APA	6.0 ^f (0.41)
6	SBE	APA	5.7 ^f (0.57)
12	BE	as sintered	9.4 ^{cd} (0.70)
12	SBE	as sintered	10.0 ^{bc} (1.55)
12	BE	APA	5.9 ^f (0.54)
12	SBE	APA	5.5 ^f (0.63)
18	BE	APA	5.7 ^f (0.91)
18	SBE	APA	5.8 ^f (1.06)

24	BE	as sintered	11.5 ^{ab} (0.67)
24	SBE	as sintered	12.9 ^a (0.76)
24	BE	APA	5.4 ^{fg} (1.53)
24	SBE	APA	5.7 ^f (1.71)

Table 2. Mean values and standard deviations for the monoclinic content (X_m) before and after ageing *in vitro*. Values marked with the same letters are not significantly different from each other (Tukey's HSD test, $\alpha = 0.05$). APA = airborne-particle abraded.

Ageing in vitro (h)	Material	Surface treatment	X_m in % (SD)
0	BE	as sintered	0.0 ^k (0.00)
0	SBE	as sintered	0.0 ^k (0.00)
0	BE	APA	5.0 ⁱ (0.22)
0	SBE	APA	5.1 ⁱ (0.48)
2	BE	as sintered	0.8 ^{jk} (0.18)
2	SBE	as sintered	1.7 ^j (1.07)
2	BE	APA	7.0 ^h (0.41)
2	SBE	APA	7.5 ^{gh} (0.19)
6	BE	as sintered	12.2 ^d (1.04)
6	SBE	as sintered	15.4 ^c (0.26)
6	BE	APA	8.0 ^{fgh} (0.34)
6	SBE	APA	8.4 ^{efg} (0.38)
10	BE	as sintered	18.1 ^b (1.03)
10	SBE	as sintered	20.9 ^a (0.47)
10	BE	APA	9.2 ^{ef} (0.44)
10	SBE	APA	9.5 ^e (0.38)

The ageing kinetics estimations obtained with regression models are presented in Fig. 3, Table 3 (*in vivo* ageing) and Table 4 (*in vitro* ageing). After 6 months *in vivo*, X_m on AS surfaces increased to 7.3% and 8.5% for finer (B-E) and coarser-grained (SB-E) 3Y-TZP specimens, respectively. The ageing process then decelerated, settling at approximately 0.23% and 0.25% per month *in vivo*. Accordingly, X_m only reached 11.5% and 13% after 24 months *in vivo* for AS B-E and SB-E samples, respectively. The *in vivo* ageing kinetics of AS specimens did not follow a clear linear trend and resembled a non-linear asymptotic growth instead (Fig. 3). Higher X_m values were observed on coarse-grained SB-E material, but these differences were not statistically significant (Table 1).

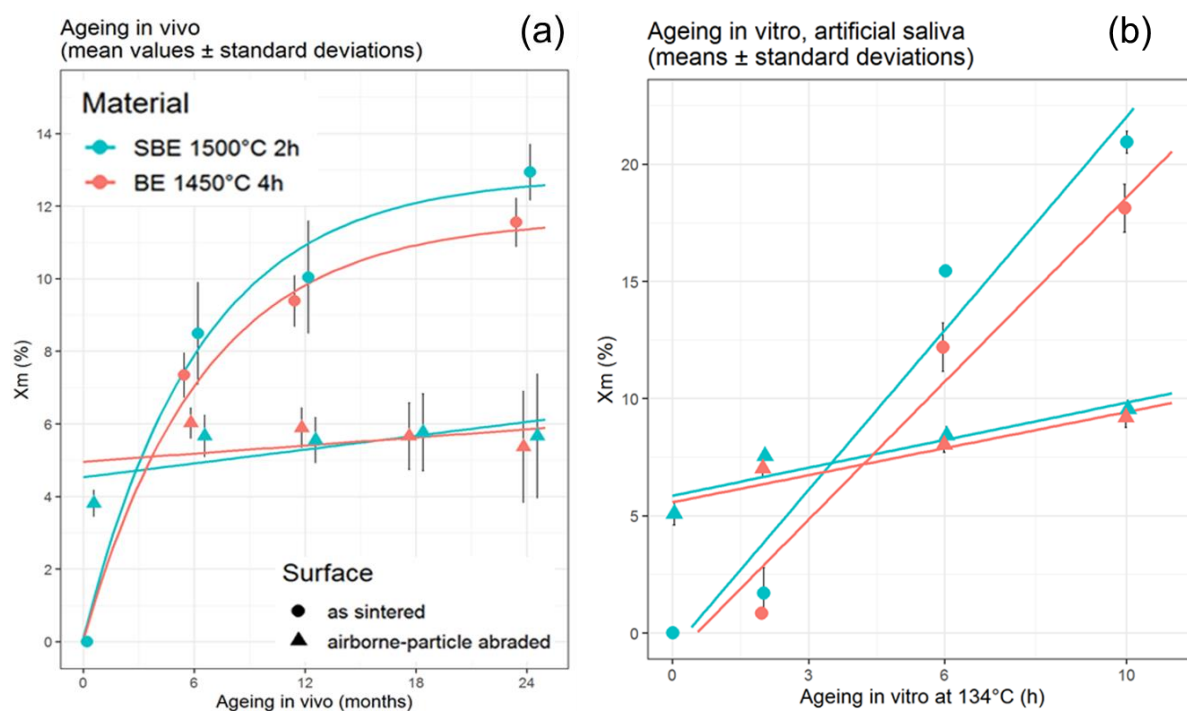


Figure 3. Ageing kinetics. Monoclinic content (X_m) and regression models after ageing *in vivo* and *in vitro*. Asymptotic regression is fitted for as-sintered groups *in vivo* and linear regression is fitted for all other groups (a). Data points are shown as means values \pm standard deviations.

Table 3. Regression analyses of the X_m progression during ageing *in vivo*. Estimated values are expressed in % change per month of ageing *in vivo*. APA = airborne-particle abraded.

	Estimate	Standard error	<i>t</i> -value	<i>p</i> -value
BE, as sintered, asymptotic regression (Residual sum of squares = 11.66)				
Asymptote	11.54	0.46	24.991	<0.0001
Intercept	0.04	0.31	0.309	0.8286
Rate parameter	-1.84	0.11	-16.144	<0.0001
SBE, as sintered, asymptotic regression (Residual sum of squares = 47.91)				
Asymptote	12.59	0.44	28.543	<0.0001
Intercept	0.08	0.31	0.250	0.8452
Rate parameter	-1.78	0.10	-17.219	<0.0001
BE, APA, linear regression (<i>F</i> =4.9 on 1 and 53 degrees of freedom, <i>p</i> =0.0311, adjusted <i>R</i> ² =0.07)				
Intercept	5.06	0.23	21.939	<0.0001
Slope	0.04	0.02	2.215	0.0311
SBE, APA, linear regression (<i>F</i> =12.17 on 1 and 59 degrees of freedom, <i>p</i> <0.0001, adjusted <i>R</i> ² =0.16)				
Intercept	4.65	0.25	18.959	<0.0001
Slope	0.06	0.02	3.489	0.0001

Table 4. Linear regression analyses of the X_m progression during ageing *in vitro*. Estimated values are expressed in % change per h of ageing *in vitro*. APA = airborne-particle abraded.

	Estimate	Standard error	t-value	p-value
BE, as sintered (F=440.1 on 1 and 18 degrees of freedom, p<0.0001, adjusted R ² =0.96)				
Intercept	-1.05	0.55	-1.896	0.0742
Slope	1.96	0.09	20.98	<0.0001
SBE, as sintered (F=400.8 on 1 and 18 degrees of freedom, p<0.0001, adjusted R ² =0.95)				
Intercept	-0.71	0.67	-1.052	0.3070
Slope	2.27	0.11	20.020	<0.0001
BE, APA (F=120.4 on 1 and 18 degrees of freedom, p<0.0001, adjusted R ² =0.86)				
Intercept	5.58	0.21	26.890	<0.0001
Slope	0.38	0.04	10.97	<0.0001
SBE, APA (85.28 on 1 and 18 degrees of freedom, p<0.0001, adjusted R ² =0.82)				
Intercept	5.86	0.25	23.08	<0.0001
Slope	0.40	0.04	9.235	<0.0001

When considering the calculated transformed zone depth (TZD), AS specimens initially aged at a rate of 0.040 μm TZD/month, but after 6 months this was followed by a considerably slower rate of 0.008 μm TZD/month. The maximum final calculated TZD after 24 months *in vivo* was 0.385 μm for the AS SB-E material (Figure 4).

APA specimen surfaces were significantly more resistant to ageing *in vivo*. Mean X_m was initially 3.8% and 4.0% for APA B-E and SB-E specimens, then increased to around 6% after 6 months and remained stable for the duration of the study. This is also evident from the diffractograms in Fig. 2a, although it is worth noting that the variability increased with time *in vivo* (Table 1). APA specimens exhibited linear ageing kinetics progressing at a rate of 0.04% per month *in vivo* (Fig. 3a, Table 3).

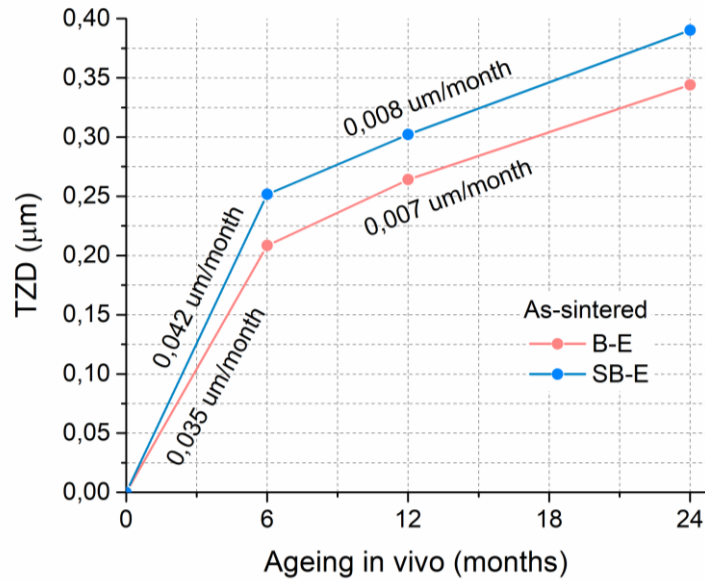


Figure 4. Transformed zone depth (TZD) of the monoclinic fraction layer as a function of *in vivo* ageing time evaluated from the X-ray data from Table 1.

Ageing *in vitro* exhibited more uniform linear ageing kinetics for both AS and APA groups, as was already indicative from the XRD diffractograms (Fig. 2c). The linear regression results are presented in Fig. 3b and Table 4. In AS groups, coarse-grained SB-E specimens aged statistically significantly faster than the fine-grained B-E, i.e., exhibiting the ageing rate of 2.27%/h and 1.96%/h, respectively. Both materials appeared to undergo an incubation period, considering that after 2 hours ageing only a barely noticeable amount of X_m (~0.8-1.7%) was detected (Fig. 2 and Table 2).

The observed *in vitro* ageing of AS samples progressed considerably faster than *in vivo*. X_m after 6 hours *in vitro* already surpassed 24 months of exposure *in vivo*, although there is also an important distinction in that the *in vivo* process appeared to be non-linear, while ageing *in vitro* was linear. APA samples exhibited low susceptibility towards the *t-m* phase transformation and were ageing at a rate of 0.4%/h *in vitro* (Fig. 3b). There was no statistically significant difference in ageing behaviour of the fine- and coarse-grained APA materials (Table 2).

3.3. Surface morphology

The ageing-induced surface changes after 24 months of *in vivo* are shown in Fig. 5. AS specimen surfaces have extensive grain uplifting due to the formation of self-accommodating martensitic variants (laths) of various orientations, as a result of the *t-m* transformation process. Martensitic variants had either intersected within a single grain, or they grew continuously from grain to grain, as reported previously [15]. In addition, microcracking within single grains and pull-outs of grain clusters were also observed. The pull-outs resembled a mixed fracture mode, with both trans- and intragranular types of fracture present.

On the APA specimen surfaces that were exposed for 24 months *in vivo*, there was no evident surface uplifting, visible martensitic variants or microcracking; however, clusters of grain pull-outs were present (Fig. 5b). The microstructural features of AS surfaces after 10 hours *in vitro* (Fig. 5c) were similar to those observed *in vivo*, but with more numerous fractures of grain clusters (Fig. 5a).

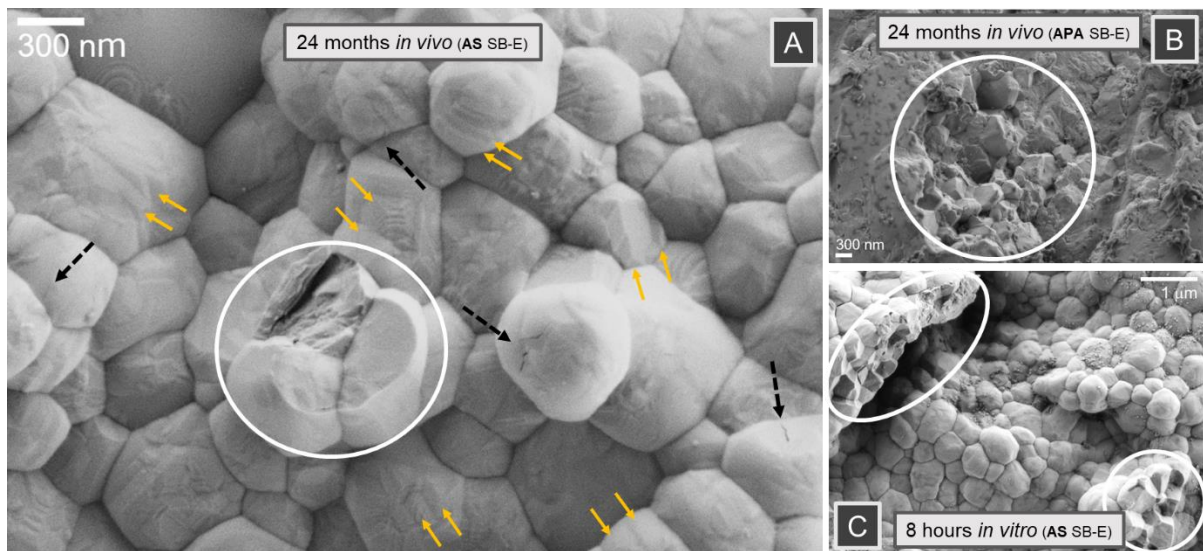


Figure 5. Surface topographies. SEM micrographs showing representative SB-E specimen surfaces from (a) AS and (b) APA groups after 24 months *in vivo*, and after 8 hours *in vitro* (c). High-magnification revealed the presence of martensitic variants (monoclinic twinning) (orange twin arrows). Additional features include trans/intragranular grain fractures, grain-pull outs (white circle) and visible microcracks on the grains (dotted black arrows) (a). APA specimen surfaces exhibited no martensitic variants nor

microcracking, but did have clusters of chipped grains (white circle) (b). These were also commonly observed on the AS specimen surfaces after ageing *in vitro* (c).

The ion-milled cross-sections were prepared with FIB-SEM to obtain insight into microstructural changes in the immediate sub-surface region. In Fig. 6, a collage of micrographs of a B-E sample is shown depicting the topmost $\sim 5 \mu\text{m}$ of sample subsurface after 24 months *in vivo*. Only the topmost few layers of grains appear to contain twin-related monoclinic variants with lath-like geometry oriented predominantly perpendicularly to the surface. Microcracks were hard to discern and were parallel to the surface. The transformed layer was homogeneous resulting in a coherent boundary between the first layer of affected grains and the unaffected bulk. The thickness of the transformed layer was around $0.5 \mu\text{m}$, which corroborates with the estimated grain size (Fig. 1b-c) and the TZD layer calculated from the XRD results (Fig. 4)

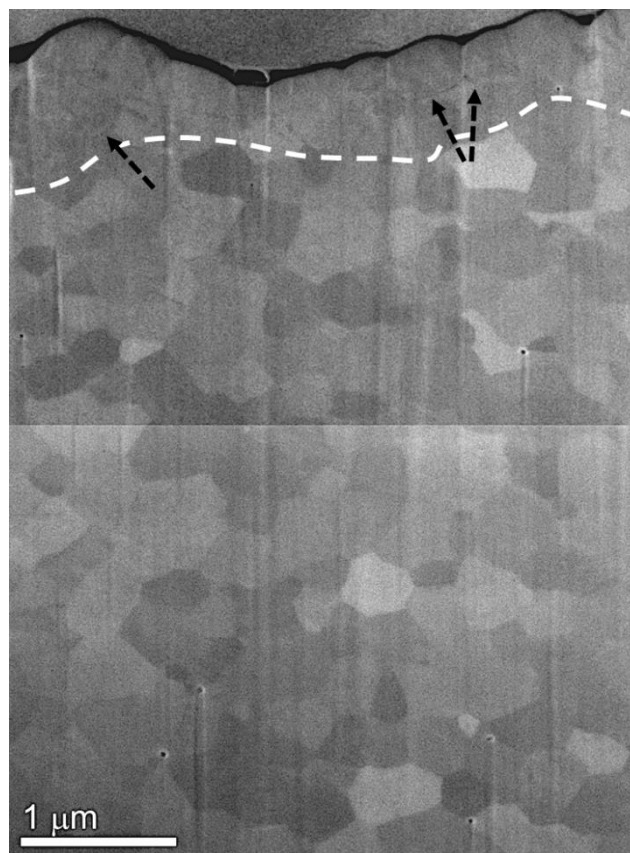


Figure 6. FIB-SEM cross-sectional collage of micrographs of a B-E specimen depicting the topmost $\sim 5 \mu\text{m}$ of the sample subsurface after 24 months *in vivo*. Black dotted arrows indicate the microcracks.

4. Discussion

The current *In vivo* ageing protocol was implemented to observe the LTD of 3Y-TZP ceramics in real clinical conditions. Disc-shaped specimens were mounted into sublingual flanges of complete denture (Fig. 1e-g). To the best of our knowledge, this study is the first to report on the 24-month-long outcome of the *in vivo* ageing of 3Y-TZP dental ceramics. The proposed ageing protocol offers several advantages compared to the accelerated artificial hydrothermal ageing in an autoclave. Firstly, ageing was studied in the natural environment of the oral cavity, where saliva flow, pH, patient habits and routine daily oral care might contribute to degradation mechanisms. The nature of the disc-shaped specimens allowed us to vary the material microstructure and surface finish, comparing the as-sintered surfaces with airborne-particle abrasion. Secondly, the removability of the disc-shaped specimens from the intraoral device allowed the use of advanced analytical tools, such as XRD and FIB-SEM, followed by re-implantation of the specimens for the predetermined observation period. The design of the study, however, did not allow us to monitor the influence of occlusal forces and wear on the ageing. The loads occurring during mastication also influence the overall performance and lifetime of zirconia restorations. It was already shown by Wei and Gremillard that applied tensile and compressive stresses accelerate the LTD process of both 3Y- and 4Y-TZP ceramics [37].

In the present study, 6 months of *in vivo* ageing already resulted in a remarkable amount of transformed monoclinic zirconia. 7.3 and 8.5% were detected on the exposed surfaces (Figs. 2 and 3, Table 1), which certainly warrants attention. Likewise, Miragaya et al. detected 4.7–7.7% of monoclinic phase after 60 days *in vivo* [46]. Obviously, the thermal cycling in the chemically aggressive wet environment in the oral cavity readily fosters *t-m* transformation on the AS surfaces of the 3Y-TZP ceramics. Previously, a similar amount of transformed monoclinic zirconia was detected on the surface of explanted HIPed and mirror-polished zirconia femoral heads after several years of service, which is much slower than what we observed in the oral cavity [28].

However, despite the initial substantial increase of the monoclinic content in the first 6 months *in vivo* (1.33% X_m /month and $\sim 0.04 \mu\text{m}$ TZD/month) (Fig. 4), the ageing rate then decelerated more than 5-times and settled at around 0.245% X_m /month ($\sim 0.0075 \mu\text{m}$ /month) for the remaining 18 months. The observed deceleration was unexpected, since Keuper et al. showed an extensive linear, continuous t - m transformation without retardation, even at 37°C and at normal pressure conditions in water or (moist) air [30]. Assuming the linear continuity of the observed ageing rate after deceleration, the observed propagation in our study is 5-times slower than the rate reported by Keuper et al [30]. The reason for the faster ageing kinetics in the latter study could be attributed to larger grain size ($\sim 700 \text{ nm}$) and lower alumina content (0.1 wt.%) of 3Y-TZP, since they used commercially available blanks sintered at a higher temperature [30]. If we extrapolated data from our study to a longer time frame, 35% X_m would be achieved after about 12 years of service *in vivo*. This is almost 3-times faster than the generally accepted *in-vitro-in-vivo* extrapolation suggested by Chevalier et al., which equals 8 hours of accelerated *in vitro* hydrothermal ageing (134°C, 2 bars, distilled water) to ~ 32 years *in vivo* [28][29]. Conversely, our *in vitro* results exhibited slower kinetics of accelerated artificial ageing, since only about 20% X_m was achieved after 10 hours (Fig. 3b). Extreme caution with such approximations is thus needed.

The non-linear, decelerating ageing kinetics we observed *in vivo* on AS specimen are not typically encountered in the t - m propagation (Figs. 3a and 4). A possible underlying reason could be the difference in nucleation and growth process between the immediate surface, which was relatively rough (Fig. 1a), and the deeper parts of the microstructure. According to the FIB-SEM analysis after 24 months *in vivo*, only a single grain layer was affected ($\sim 0.5 \mu\text{m}$). The change in kinetics would then have occurred at the depth of 0.2-0.25 μm , (Fig. 4), which is approximately one half of the grain size. On the other hand, the build-up of oral biofilm (plaque) could have affected the ageing kinetics if such a deposit somehow hindered the diffusion of water species to the 3Y-TZP surface and the propagation into the bulk. However, the limitation in diffusion would only be relevant for the t - m transformation on the immediate

surface. It was already shown previously that the progression of transformation into the bulk does not require a constant, diffusion-controlled supply of water, since the transformation appears to be a self-sustaining autocatalytic process [10][30][12]. Moreover, if biofilm had an effect, this should also be apparent in our second *in vivo* study [ref in vivo paper 2], but this was not the case. Data from our second study corresponded very well to the linear ageing kinetics. It is unclear why *in vivo* ageing in the present study deviated from the widely reported linearity.

APA of specimen surfaces was highly effective in making 3Y-TZP more ageing resistant both *in vivo* and *in vitro*. The observations corroborate with previous reports, where the evolved compressive micro-residual stresses [21,32] as a result of mechanical surface damage are responsible for the initial, slower ageing. These residual stresses can be related to the observed reversed intensities of the tetragonal doublet peaks $(002)_t$ and $(110)_t$ (Figs. 2b and d) as a result of ferroelastic domain switching. This is known to occur with an externally applied stress and can exert substantial coercive stresses [38][39]. Alternatively, or hand in hand, the compressive stresses evolve as a consequence of the *t-m* [40] and/or the *t-r* (*r* as rhombohedral phase) transformation [41]. However, when the stresses are annihilated by the ageing process, the speed of ageing kinetics will accelerate back to the rate seen in as-sintered specimens [11]. The duration of *in vivo/in vitro* exposure in this study was insufficient for this transition to occur. Cotič et al. previously showed that the transition in ageing kinetics for the B-E material sintered at 1500°C for 2 hours occurred at 55% X_m (corresponding to ~6 μm of TZD). Considering the material type and ageing conditions in the present study, this would be achieved after more than 110 years *in vivo* or after ~135 hours *in vitro*.

5. Conclusion

Biomedical grade 3Y-TZP dental ceramics with 0.25 wt.% alumina content were exposed to the oral environment for 24 months. The as-sintered materials' surfaces were susceptible to ageing, which proceeded with non-linear growth kinetics. Fine- and coarse-grained variants did not exhibit statistically significant differences in ageing behaviour *in vivo* regardless of

surface treatment, but the coarse-grained as-sintered material did age statistically significantly faster than the fine-grained material *in vitro*. After 2 years of *in vivo* exposure, the thickness of the transformed layer was $\sim 0.385 \mu\text{m}$. Intragranular microcracks and grain pull-outs were also observed. The *t-m* progression was slow, but assuming linear ageing kinetics after deceleration ($0.245\% X_m/\text{month}$; $\sim 0.0075 \mu\text{m}/\text{month}$), 35% of the monoclinic fraction would be achieved in less than 12 years of service. This is almost 3-times faster than the generally accepted *invitro-in-vivo* extrapolation for the lifetime prediction. Air-particle-abrasion substantially suppressed LTD.

Acknowledgements

This work was supported by the Slovenian Research Agency funding through research project Towards reliable implementation of monolithic zirconia dental restorations (J2-9222) and research program Ceramics and complementary materials for advanced engineering and biomedical applications (P2-0087). The authors are grateful to Prof. Michael V. Swain for continuous motivation and valuable discussions.

References

- [1] Denry I, Kelly JR. State of the art of zirconia for dental applications. *Dent Mater* 2008;24:299–307. <https://doi.org/10.1016/j.dental.2007.05.007>.
- [2] Garvie R, Hannink R, Pascoe R. Ceramic steel? *Nature* 1975;258:703–4.
- [3] Gupta TK, Lange FF, Bechtold JH. Effect of stress-induced phase transformation on the properties of polycrystalline zirconia containing metastable tetragonal phase. *J Mater Sci* 1978;13:1464–70. <https://doi.org/10.1007/BF00553200>.
- [4] Zhang F, Batuk M, Hadermann J, Manfredi G, Mari??n A, Vanmeensel K, et al. Effect of cation dopant radius on the hydrothermal stability of tetragonal zirconia: Grain

- boundary segregation and oxygen vacancy annihilation. *Acta Mater* 2016;106:48–58.
<https://doi.org/10.1016/j.actamat.2015.12.051>.
- [5] Lughì V, Sergo V. Low temperature degradation -aging- of zirconia: A critical review of the relevant aspects in dentistry. *Dent Mater* 2010;26:807–20.
<https://doi.org/10.1016/j.dental.2010.04.006>.
- [6] Kobayashi K, Kuwajima H, Masaki T. Phase change and mechanical properties of ZrO₂-Y₂O₃ solid electrolyte after ageing. *Solid State Ionics* 1981;3–4:489–93.
[https://doi.org/10.1016/0167-2738\(81\)90138-7](https://doi.org/10.1016/0167-2738(81)90138-7).
- [7] Chevalier J, Gremillard L, Virkar A V., Clarke DR. The Tetragonal-Monoclinic Transformation in Zirconia: Lessons Learned and Future Trends. *J Am Ceram Soc* 2009;92:1901–20. <https://doi.org/10.1111/j.1551-2916.2009.03278.x>.
- [8] Lawson S. Environmental degradation of zirconia ceramics. *J Eur Ceram Soc* 1995;15:485–502. [https://doi.org/10.1016/0955-2219\(95\)00035-S](https://doi.org/10.1016/0955-2219(95)00035-S).
- [9] Kosmač T, Kocjan A. Ageing of dental zirconia ceramics. *J Eur Ceram Soc* 2012;32:2613–22. <https://doi.org/10.1016/j.jeurceramsoc.2012.02.024>.
- [10] Keuper M, Eder K, Berthold C, Nickel KG. Direct evidence for continuous linear kinetics in the low-temperature degradation of Y-TZP. *Acta Biomater* 2013;9:4826–35.
<https://doi.org/10.1016/j.actbio.2012.08.032>.
- [11] Cotič J, Jevnikar P, Kocjan A. Ageing kinetics and strength of airborne-particle abraded 3Y-TZP ceramics. *Dent Mater* 2017;33.
<https://doi.org/10.1016/j.dental.2017.04.014>.
- [12] Muñoz-Tabares J a., Jiménez-Piqué E, Anglada M. Subsurface evaluation of hydrothermal degradation of zirconia. *Acta Mater* 2011;59:473–84.
<https://doi.org/10.1016/j.actamat.2010.09.047>.
- [13] Yoshimura M, Noma T, Kawabata K, Sōmiya S. Role of H₂O on the degradation

- process of Y-TZP. *J Mater Sci Lett* 1987;6:465–7.
<https://doi.org/10.1007/BF01756800>.
- [14] Chevalier J. What future for zirconia as a biomaterial? *Biomaterials* 2006;27:535–43.
<https://doi.org/10.1016/j.biomaterials.2005.07.034>.
- [15] Deville S, Chevalier J. Martensitic Relief Observation by Atomic Force Microscopy in Yttria-Stabilized Zirconia. *J Am Ceram Soc* 2003;86:2225–7.
- [16] Haraguchi K, Sugano N, Nishii T, Miki H, Oka K, Yoshikawa H. Phase transformation of a zirconia ceramic head after total hip arthroplasty. *J Bone Jt Surg - Ser B* 2001;83:996–1000. <https://doi.org/10.1302/0301-620X.83B7.12122>.
- [17] Masonis JL, Bourne RB, Ries MD, McCalden RW, Salehi A, Kelman DC. Zirconia femoral head fractures: A clinical and retrieval analysis. *J Arthroplasty* 2004;19:898–905. <https://doi.org/10.1016/j.arth.2004.02.045>.
- [18] Hallmann L, Mehl A, Ulmer P, Reusser E, Stadler J, Zenobi R, et al. The influence of grain size on low-temperature degradation of dental zirconia. *J Biomed Mater Res - Part B Appl Biomater* 2012;100 B:447–56. <https://doi.org/10.1002/jbm.b.31969>.
- [19] Xiong Y, Fu Z, Pouchly V, Maca K, Shen Z. Preparation of Transparent 3Y-TZP Nanoceramics with No Low-Temperature Degradation. *J Am Ceram Soc* 2014;97:1402–6. <https://doi.org/10.1111/jace.12919>.
- [20] Samodurova A, Kocjan A, Swain M V, Kosmač T. The combined effect of alumina and silica co-doping on the ageing resistance of 3Y-TZP bioceramics. *Acta Biomater* 2015;11:477–87. <https://doi.org/10.1016/j.actbio.2014.09.009>.
- [21] Kosmač T, edomir Oblak Č, Jevnikar P, Funduk N, Marion L. Strength and Reliability of Surface Treated Y - TZP Dental Ceramics. *J Biomed Mater Res (Appl Biomater)* 2000;53:304–13. [https://doi.org/10.1002/1097-4636\(2000\)53:43.0.CO;2-S](https://doi.org/10.1002/1097-4636(2000)53:43.0.CO;2-S).
- [22] Kosmac T, Oblak C, Jevnikar P, Funduk N, Marion L. The effect of surface grinding

- and sandblasting on flexural strength and reliability of Y-TZP zirconia ceramic. *Dent Mater* 1999;15:426–33.
- [23] Chintapalli RK, Marro FG, Jimenez-Pique E, Anglada M. Phase transformation and subsurface damage in 3Y-TZP after sandblasting. *Dent Mater* 2013;29:566–72. <https://doi.org/10.1016/j.dental.2013.03.005>.
- [24] Cotič J, Jevnikar P, Kocjan A, Kosmač T. Complexity of the relationships between the sintering-temperature-dependent grain size, airborne-particle abrasion, ageing and strength of 3Y-TZP ceramics. *Dent Mater* 2016;32:510–8. <https://doi.org/10.1016/j.dental.2015.12.004>.
- [25] Caravaca CF, Flamant Q, Anglada M, Gremillard L, Chevalier J. Impact of sandblasting on the mechanical properties and aging resistance of alumina and zirconia based ceramics. *J Eur Ceram Soc* 2018;38:915–25. <https://doi.org/10.1016/j.jeurceramsoc.2017.10.050>.
- [26] Cattani-Lorente M, Scherrer SS, Ammann P, Jobin M, Wiskott HWA. Low temperature degradation of a Y-TZP dental ceramic. *Acta Biomater* 2011;7:858–65. <https://doi.org/10.1016/j.actbio.2010.09.020>.
- [27] Swain M V. Impact of oral fluids on dental ceramics: What is the clinical relevance? *Dent Mater* 2014;30:33–42. <https://doi.org/10.1016/j.dental.2013.08.199>.
- [28] Chevalier J, Gremillard L, Deville S. Low-Temperature Degradation of Zirconia and Implications for Biomedical Implants. *Annu Rev Mater Res* 2007;37:1–32. <https://doi.org/10.1146/annurev.matsci.37.052506.084250>.
- [29] Chevalier J, Gremillard L. Ceramics for medical applications: A picture for the next 20 years. *J Eur Ceram Soc* 2009;29:1245–55. <https://doi.org/10.1016/j.jeurceramsoc.2008.08.025>.
- [30] Keuper M, Berthold C, Nickel KG. Long-time aging in 3 mol.% yttria-stabilized

- tetragonal zirconia polycrystals at human body temperature. *Acta Biomater* 2014;10:951–9. <https://doi.org/10.1016/j.actbio.2013.09.033>.
- [31] Miragaya LM, Guimarães RB, Othávio R, Assunção D, Botelho S, Guilherme J, et al. Effect of intra-oral aging on t→m phase transformation, microstructure, and mechanical properties of Y-TZP dental ceramics. *J Mech Behav Biomed Mater* 2017;72:14–21. <https://doi.org/10.1016/j.jmbbm.2017.04.014>.
- [32] Mendelson M. Average grain size in polycrystalline ceramics. *J Am Ceram Soc* 1969;52:443–6.
- [33] Garvie R, Nicholson P. Phase analysis in zirconia systems. *J Am Ceram ...* 1972;303–5. <https://doi.org/10.1111/j.1151-2916.1972.tb11290.x>.
- [34] Bučevac D, Kosmač T, Kocjan A. The influence of yttrium-segregation-dependent phase partitioning and residual stresses on the aging and fracture behaviour of 3Y-TZP ceramics. *Acta Biomater* 2017;62:306–16. <https://doi.org/10.1016/j.actbio.2017.08.014>.
- [35] Ruiz L, Readey MJ. Effect of heat-treatment on grain size, phase assemblage, and mechanical properties of 3 mol% Y-TZP. *J Am Ceram Soc* 1996;79:2331–40. <https://doi.org/10.1111/j.1151-2916.1996.tb08980.x>.
- [36] Bowman KJ, Chen I -W. Transformation Textures in Zirconia. *J Am Ceram Soc* 1993;76:113–22. <https://doi.org/10.1111/j.1151-2916.1993.tb03696.x>.
- [37] Wei C, Gremillard L. The influence of stresses on ageing kinetics of 3Y- and 4Y-stabilized zirconia. *J Eur Ceram Soc* 2018;38:753–60. <https://doi.org/10.1016/j.jeurceramsoc.2017.09.044>.
- [38] Virkar A, Matsumoto R. Ferroelastic domain switching as a toughening mechanism in tetragonal zirconia. *J Am Ceram Soc* 1986;69:C-224-C–226.
- [39] Kocjan A, Abram A, Dakskobler A. Impact strengthening of 3Y-TZP dental ceramic

root posts. *J Eur Ceram Soc* 2020;40:4765–73.

<https://doi.org/10.1016/j.jeurceramsoc.2020.02.040>.

- [40] Chintapalli RK, Mestra Rodriguez A, Garcia Marro F, Anglada M. Effect of sandblasting and residual stress on strength of zirconia for restorative dentistry applications. *J Mech Behav Biomed Mater* 2014;29:126–37.

<https://doi.org/10.1016/j.jmbbm.2013.09.004>.

- [41] Hasegawa H. Rhombohedral phase produced in abraded surfaces of partially stabilized zirconia (PSZ). *J Mater Sci Lett* 1983;2:91–3.